Available online at www.sciencedirect.com

SciVerse ScienceDirect

Acta Materialia 60 (2012) 6862–6868

Acta MATERIALIA

www.elsevier.com/locate/actamat

Indentation size effect and shear transformation zone size in a bulk metallic glass in two different structural states

In-Chul Choi [a], Yakai Zhao [a], Yong-Jae Kim [a], Byung-Gil Yoo [a], Jin-Yoo Suh [b], Upadrasta Ramamurty [c], Jae-il Jang [a,*]

[a] Division of Materials Science and Engineering, Hanyang University, Seoul 133-791, Republic of Korea
[b] High Temperature Energy Materials Center, Korea Institute of Science and Technology, Seoul 136-791, Republic of Korea
[c] Department of Materials Engineering, Indian Institute of Science, Bangalore 560 012, India

Received 7 July 2012; received in revised form 25 August 2012; accepted 27 August 2012
Available online 22 September 2012

Abstract

The existence of an indentation size effect (ISE) in the onset of yield in a Zr-based bulk metallic glass (BMG) is investigated by employing spherical-tip nanoindentation experiments. Statistically significant data on the load at which the first pop-in in the displacement occurs were obtained for three different tip radii and in two different structural states (as-cast and structurally relaxed) of the BMG. Hertzian contact mechanics were employed to convert the pop-in loads to the maximum shear stress underneath the indenter. Results establish the existence of an ISE in the BMG of both structural states, with shear yield stress increasing with decreasing tip radius. Structural relaxation was found to increase the yield stress and decrease the variability in the data, indicating "structural homogenization" with annealing. Statistical analysis of the data was employed to estimate the shear transformation zone (STZ) size. Results of this analysis indicate an STZ size of ~25 atoms, which increases to ~34 atoms upon annealing. These observations are discussed in terms of internal structure changes that occur during structural relaxation and their interaction with the stressed volumes in spherical indentation of a metallic glass.

Keywords: Bulk metallic glass; Nanoindentation; Indentation size effect; Shear transformation zone; Yield strength

1. Introduction

The small-scale strength and plasticity of metals and alloys has been a topic of active research over the past two decades. It is now well recognized that size plays an important role in the mechanical properties, especially at the submicrometer scale with "smaller typically being stronger". One well-known manifestation of this phenomenon is the indentation size effect (ISE), which causes the measured hardness, H, to increase with decreasing indentation depth, h, for a sharp indenter and decreasing indenter radius, R, for a spherical indenter [1]. Strain gradient plasticity, which invokes the concept of geometrically necessary dislocations within the framework of Taylor hardening, is popular for rationalizing ISE [1,2]. In a recent study, Shim et al. [3], who performed spherical indentation on single-crystal Ni, found that the yield stress (which manifests as a sudden displacement excursion or "pop-in" at the elastic-to-plastic transition) increases as R decreases. This phenomenon was rationalized by recourse to the connection between the volume of the highly stressed material underneath the indenter and the distribution of mobile dislocations within it [3,4]. It was argued that as R decreases, the likelihood of the stressed zone containing the required preexisting mobile dislocations gets lowered, resulting in the elevation of yield stress. For a very small indenter, the stressed zone may be dislocation-free and thus stresses that are close to theoretical strength are required for yielding [3,4].

* Corresponding author.
E-mail address: jijang@hanyang.ac.kr (J.-i. Jang).

1359-6454/$36.00
http://dx.doi.org/10.1016/j.actamat.2012.08.061

Hitherto, all the mechanisms suggested as possible sources for ISE are based on dislocation-mediated plasticity. Naturally, an important scientific question to consider is: would a material that does not rely on such processes also exhibit ISE? An example of such a material is metallic glass, the plasticity of which occurs through atomic cluster shearing (the clusters are often referred to as shear transformation zones (STZs)), and subsequent localization of flow into narrow bands ("shear bands") at low temperatures and high stresses [5–7]. In addition to being scientifically intriguing, there has been considerable technological interest in these materials as they can be processed in bulk form. While there are several reports on ISE in H of various bulk metallic glasses (BMGs) (see Ref. [8] for a summary), only Bei et al. [9] have examined the ISE on the first pop-in stress through nanoindentation tests with spherical tips of different R on a Zr-based BMG. However, because their data sets were rather limited in size, about 20 for each condition, a definitive conclusion on the existence of ISE could not be drawn. In this work, we overcome this problem by generating large data sets (about 120 in each case). In addition, the BMG's response was examined in both as-cast and annealed states in order to study the effect of structural relaxation, which generally increases the yield stress, on ISE. Importantly, these results were utilized to estimate the size of STZs through a statistical analysis of the data. Variation of the STZ size with annealing is discussed in terms of the structural changes affected by relaxation.

2. Experimental

A ~7 mm diameter and ~70 mm long rod of Zr-based BMG, $Zr_{52.5}Cu_{17.9}Ni_{14.6}Al_{10}Ti_5$ (commercial designation: Vit 105) was examined in this work. The glass-transition temperature (T_g) of this alloy is ~673 K [10]. The glass was structurally relaxed by annealing at 630 K, which corresponds to ~$0.93T_g$, for 3600 s. X-ray diffraction spectra obtained from both the as-cast and annealed specimens (not shown here) suggests that both the materials are X-ray amorphous. Further, the time–temperature combination employed for the annealing treatment is such that it produces a fully or almost-fully relaxed atomic configuration on the basis of the reported relaxation kinetics of a similar Zr-based metallic glass [11]. Yet it was far below the temperature for initiating crystallization of the glass. Thus, it is reasonable to assume that the structural relaxation treatment only alters the structural state of the BMG but does not lead to crystallization.

Nanoindentation experiments were conducted at room temperature using a Nanoindenter-XP (formerly MTS; now Agilent, Oak Ridge, TN) instrument with three different spherical indenter tips having tip radii, R, of 2.91, 5.75 and 31.5 μm. Each tip radius was calibrated, both before and after the experiments, by Hertzian contact analysis [12] of indentations made on fused quartz. Tests were conducted in load-control mode with a fixed loading rate of 1 mN s^{-1}. More than 120 tests were conducted for each testing condition so as to obtain statistically significant data sets. In all experiments, thermal drift was maintained to be <0.05 nm s^{-1}.

3. Results

3.1. ISE in as-cast state

Fig. 1 shows representative load–displacement (P–h) curves for the three indenters. Here, the data are normalized with respective peak values. The actual peak loads (P_{max}) were 15, 60 and 300 mN for tip radii of 2.91, 5.75 and 31.5 μm, respectively. Each curve exhibits a pop-in where the P–h relation starts to deviate from that expected from Hertzian elastic contact mechanics, given by [12]:

$$P = \frac{4}{3}E_r\sqrt{R}\cdot h^{\frac{3}{2}}, \tag{1a}$$

and

$$\frac{E_s}{1-\nu_s^2} = \left(\frac{1}{E_r} - \frac{1-\nu_i^2}{E_i}\right)^{-1}, \tag{1b}$$

where E and ν are the elastic modulus and Poisson's ratio, with the subscripts s and i indicating the sample and the indenter, respectively. The reduced modulus, E_r, accounts for the fact that elastic deformations occur in both the indenter and the sample. Since a diamond tip is used, $E_i = 1141$ GPa and $\nu_i = 0.07$ [13]. By fitting the loading part of the P–h curves with Eq. (1), the indentation modulus of the samples, $E_s/(1-\nu_s^2)$, was estimated to be ~100–110 GPa, which is in an agreement with the reported value for this BMG (~103 GPa based on $E_s = 89$ GPa and $\nu_s = 0.37$) [14]. In addition, the loading and unloading segments of the P–h curves, wherein P_{max} kept lower than the first pop-in load, completely overlap, with no residual indentation depth whatsoever. This indicates that the deformation is purely elastic prior to the first pop-in.

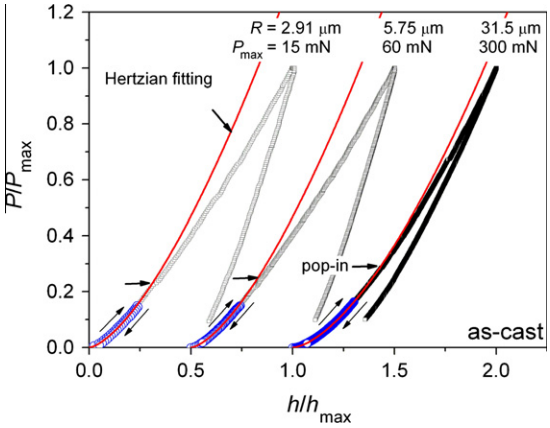

Fig. 1. Representative load vs. depth of penetration curves for the as-cast sample. Here, for comparison purposes, the data are normalized with respective maximum values, which are given in the figure.

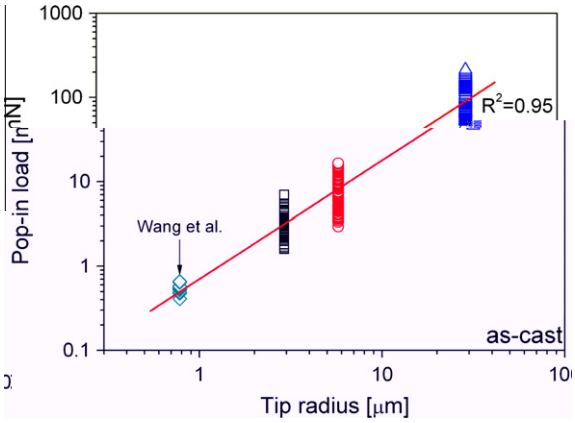

Fig. 2. Variation of the first pop-in loads with the indenter radius in the as-cast alloy. Data reported by Wang et al. [15] for the same alloy and with a tip radius of 780 nm is also plotted for comparison purposes. The solid red line is a power-law (Eq. (2)) fit to the data.

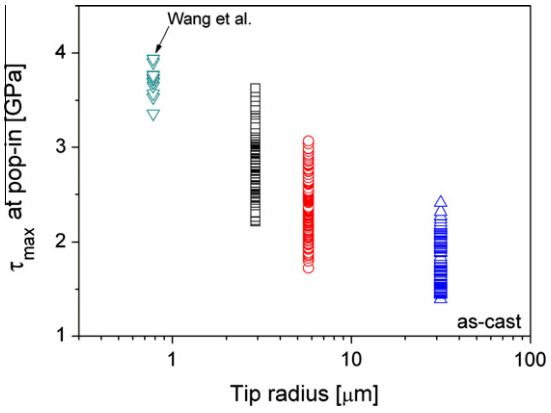

Fig. 3. Variation of the maximum shear stress, estimated from the first pop-in load using Eq. (3), as a function of indenter radius for the as-cast alloy.

Fig. 2 summarizes the dependence of the first pop-in load, P_I, on tip radius R. In addition, the data obtained by Wang et al. [15], wherein a tip of 780 nm radius was employed on nominally the same glass as that used in the current study and at the same loading rate (1 mN s^{-1}), is also plotted. Note that Wang et al.'s dataset is comparatively small (~30), resulting in a relatively small range of P_I. The range, average and standard deviations of the each data set are summarized in Table 1. An obvious trend is seen; all of them increase monotonically with increasing R. The data appears to be described well with a power law:

$$P_I = 0.7 \times R^{1.407}. \quad (2)$$

The maximum shear stress at the first-pop-in, τ_{max}, represents the critical shear strength for the onset of plasticity in the indented material. In spherical indentation, τ_{max}, occurs at a distance approximately half the contact radius directly below the rotational axis of the contact and is given as [12]:

$$\tau_{max} = 0.31 p_0 = 0.31\left(\frac{3}{2}p_m\right) = 0.31\left(\frac{6E_r^2}{\pi^3 R^2}P_I\right)^{\frac{1}{3}}, \quad (3)$$

where p_0 and p_m are maximum and mean pressures of the contact, respectively. P_I data plotted in Fig. 2 is converted into τ_{max} with the aid of Eq. (3), as displayed in Fig. 3, with details such as range, average and variance listed in Table 1. Again, size dependence emerges, while the average value of τ_{max} increases as R gets smaller, whereas the variance (given by the ratio of standard deviation and the average value) increases with R. These trends are similar to those reported by Shim et al. [3] for the ISE on yield of single-crystal Ni. It is worth noting again that Bei et al. [9] also estimated τ_{max} for various indenters with different R, but did not find a clear trend. In their case the upper bound of τ_{max} remained invariant with R, whereas the lower bound decreased with increasing R.

3.2. ISE in annealed sample

Annealing of the as-cast metallic glasses at temperatures below their T_g causes free volume annihilation and thus an increase in atomic packing density [5]. This process is often referred to as structural relaxation and alters the mechanical behavior of the BMG dramatically [10,16,17]. The change in P_I of the annealed sample with R is shown in Fig. 4. The inset image of Fig. 4 shows that, for $R = 31.5$ μm, deformation is purely elastic up to $P_{max} = 500$ mN, which is the maximum load capacity of the equipment available to us. Therefore, we could not get P_I data for this R. However, data obtained with the other two indenters clearly show that trend in P_I vs. R on the structurally relaxed alloy is similar to that seen in

Table 1
Summary of first pop-in loads and stresses. Average and standard deviation are abbreviated as AVE and STD, respectively.

	Tip radius, R (μm)	First pop-in load, P_I			First pop-in stress, τ_{max}		
		Measured full range (mN)	AVE & STD (mN)	STD/AVE (%)	Measured full range (GPa)	AVE & STD (GPa)	STD/AVE (%)
As-cast	2.91	1.60–7.00	3.44 ± 1.11	32.3	2.21–3.63	2.83 ± 0.30	10.6
	5.75	2.94–16.6	7.86 ± 3.07	39.1	1.72–3.07	2.35 ± 0.30	12.8
	31.5	46.7–215	107 ± 48.4	45.2	1.39–2.41	1.80 ± 0.26	14.4
Annealed	2.91	3.87–12.6	9.08 ± 1.70	18.7	2.97–4.40	3.94 ± 0.27	6.85
	5.75	10.6–27.1	15.8 ± 3.30	20.9	2.67–3.65	3.04 ± 0.20	6.58

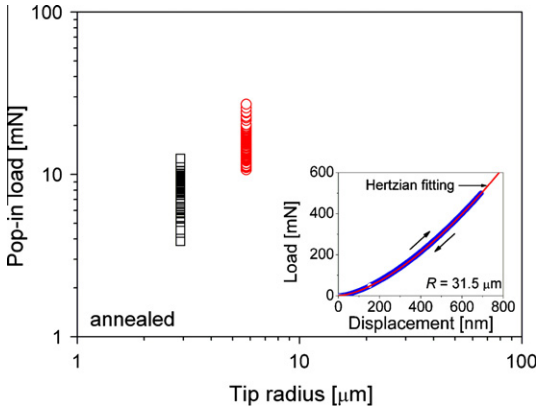

Fig. 4. Variation in the first pop-in load with the indenter radius in the structurally relaxed alloy. Inset shows a representative P–h curve obtained with an indenter whose tip radius is 31.5 μm.

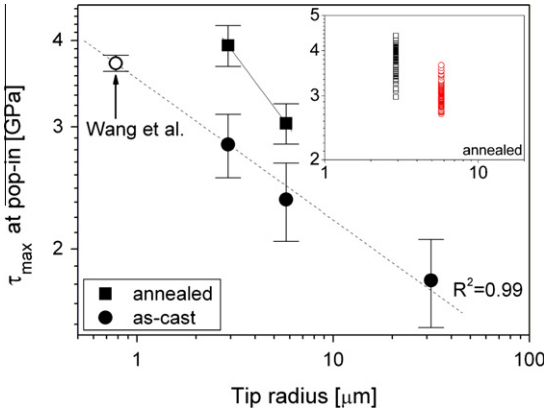

Fig. 5. Variations in the maximum shear stress at first pop-in with the tip radius for both as-cast and annealed BMG. Original full dataset for the annealed sample is provided in the inset. While a proper fitting is not possible for annealed sample (because only two R values are available), the data for as-cast sample are described very well with a power-law (whose exponent is approximately −0.2).

the as-cast sample. Variations in the average values of τ_{max} with R for both as-cast and annealed sample are plotted in Fig. 5. The original dataset for the annealed sample is displayed in the inset. While an ISE in τ_{max} (i.e. increasing τ_{max} with reducing R) is evident for both alloys, two distinct features of the annealed alloy vis-à-vis the as-cast alloy are noteworthy: (i) for a given R, P_I is much higher (~30 to 40%) in the annealed sample as compared to that in the as-cast alloy; (ii) the variability in the data for the structurally relaxed alloy is substantially smaller than that recorded in the as-cast alloy. Additionally, annealing appears to eliminate the size dependence of the variability, i.e. the variance in τ_{max} of the structurally relaxed alloy is independent of R.

4. Discussion

4.1. Influence of structural relaxation on ISE

Shim et al. [3] rationalize the ISE in crystalline Ni on the basis of the relative sizes of the highly stressed zone underneath the indenter and the average spacing between mobile dislocations. As the indenter gets smaller, the probability for finding pre-existing mobile dislocations in the highly-stressed volume decreases, which in turn elevates the flow stress of the metal.

In metallic glasses, the unit carriers of plasticity are STZs and regions with high free volume (or low local density) are the preferred locations for the STZ activation. Since STZs are mobile dislocation analogues, an approach that is similar to that employed by Shim et al. [3] can be adopted for understanding the mechanism of the ISE noted in Figs. 3 and 5. However, cognizance of the intrinsic difference between STZs and dislocations is a must here. Unlike dislocations, STZs are not structural defects and hence they do not pre-exist in the glass before deformation. The structure of metallic glasses is inherently inhomogeneous in nature due to the disordered arrangement of atoms. As a result, wide fluctuations in local atomic packing densities can be expected. This in turn results in a statistical distribution of free volume, which exerts a strong influence on elastic and plastic properties. For example, recent studies show that the local nanoscale elastic modulus in a metallic glass can vary significantly [18]. With respect of plastic deformation, STZs occur at high free volume sites and then percolate to form a shear band along the maximum shear stress direction. Thus, as R increases and the volume of material being sampled during indentation becomes larger, the probability of finding the weaker region is higher and hence lower stresses are needed to initiate plasticity. In this context, the potential energy landscape (PEL) perspective [19,20] is noteworthy. The kinetics of an elastic-to-plastic transition in metallic glasses can be separated into slow α and fast β relaxation processes, which are related to irreversible and reversible hopping of atomic clusters, respectively. With decreasing "volume," the number of α events increases but their amplitude decreases, both of which are strong functions of the size and density of isolated STZs since the events may be directly linked to the collapse of the STZ–matrix coherency condition. In contrast, the amplitude of reversible β events is more or less independent of the volume size. Additionally, STZs can result in long-range internal stress, such as an Eshelby back-stress [20], which is not the case with glide of mobile dislocations. These internal stresses may also have a role to play in the observed ISE, although we do not yet have a clear picture as to the precise nature of this.

The observed trends in the data of both P_I and τ_{max}, summarized in Table 1 for both the as-cast and the annealed alloys, can be also rationalized by recourse to the above STZ-free volume concept. During sub-T_g annealing of metallic glasses, atoms in the "compressed" regions (i.e. closer-packed regions) move slightly so as to relax internal stresses by redistributing them at the expense of the relatively more "open" regions next to the atoms. This "structural relaxation" reduces the number of "liquid like" (i.e. regions with high local free volume concentrations)

potential sites for the STZ operation, and effectively elevates the flow stress of the glass. This behavior explains why the annealed sample exhibits a higher τ_{max} at the first pop-in on average as well as lower bound (or threshold). Another important feature in Table 1 is the variance in τ_{max} of the annealed sample vis-à-vis the as-cast sample. It is well understood that structural relaxation leads to "redistribution" of free volume, making the overall free volume content less and its distribution much narrower. For example, X-ray scattering measurements suggest that structural inhomogeneity in the glass decreases by annealing the glass below its T_g [21]. A natural consequence of such "homogenization" is the reduction in the variability for STZ activation stresses, which is what is seen in the experimental results of this work.

Before closing this section on the ISE, it is important to note the following deficiency in the $\tau_{\max}$ vs. R analysis. As mentioned earlier, there is a statistical distribution in the free volume in the material. This, combined with the stress gradients that are inevitable in contact mechanics problems, imply that yielding will occur in regions where the stress-free volume combination is optimum. Thus, the first STZ does not need to occur at the specific location of $\tau_{\max}$. Instead, it will tend to occur at the place where the combination of internal structure and applied indentation stress is the most favorable. An analysis that combines the inhomogeneous stress distribution with the stochastic nature of the material is desirable in future, especially when description of the actual distribution of the weaker region becomes possible.

4.2. Size of the STZs

An additional information, which is vital in the context of physics of plastic deformation in metallic glasses, that can be obtained from the experimental data of this work is the size of STZs involved in yielding. Based on the thermally activated, stress-assisted behavior of STZs, in an earlier study we have suggested a way to estimate the STZ size as a function of the strain rate [22], of which a brief summary is presented below.

In the cooperative shear model (CSM) model of Johnson and Samwer [23], yielding is determined by the cooperative shear motion of STZs and hence intrinsically depends on activation volume V^*. By differentiation of the activation energy in the CSM model, the relation between the STZ volume Ω and activation volume V^* can be obtained as:

$$\Omega = \frac{\tau_{C0}}{6CG\gamma_C^2\zeta\left(1-\frac{\tau_{CT}}{\tau_{C0}}\right)^{\frac{1}{2}}}V^*, \tag{4}$$

where G is the shear modulus (= 32.5 GPa for the BMG under consideration here), τ_{CT} and τ_{C0} are the threshold shear strengths at T and 0 K, respectively, γ_C is the critical shear strain ($=\tau_{CT}/G$), and constants $C \approx 1/4$ and $\zeta \approx 3$ [23]. With the data from 30 different metallic glasses, Johnson and Samwer [23] arrived at a scaling law for their flow stress as:

$$\gamma_C = \frac{\tau_{CT}}{G} = \gamma_{C0} - \gamma_{C1}\left(\frac{T}{T_g}\right)^M, \tag{5}$$

where $\gamma_{C0} = 0.036 \pm 0.002$, $\gamma_{C1} = 0.016 \pm 0.002$ and $M = 0.62 \pm 0.2$. Therefore, for a given G and T_g, both τ_{CT} and τ_{C0} (i.e. $\gamma_{C0}G$ at $T = 0$ K) of a metallic glass can be estimated from this constitutive equation. Collectively, if V^* of the pop-in event can be estimated through nanoindentation tests, the size of STZ involved in the yielding can be determined according to Eq. (4). It is worth noting that, in Eq. (4), G does not affect the calculated STZ volume because both τ_{CT} and τ_{C0} are linearly proportional to it.

The cumulative distribution of τ_{max} is illustrated in Fig. 6. Schuh and Lund [24] suggested that the thermally-assisted and stress-biased yielding always exhibits a spread in the yield strengths. This is because the thermal noise sometimes favors yielding and sometimes works against it. On this basis, the cumulative distribution function of pop-in events (i.e. cumulative probability in Fig. 6) can be described as a function of the shear stress beneath the indenter, τ [24]:

$$f = 1 - \exp\left[-\frac{kT\dot{\gamma}_0}{V^*(d\tau/dt)}\exp\left(-\frac{\Delta F^*}{kT}\right)\exp\left(\frac{\tau V^*}{kT}\right)\right], \tag{6}$$

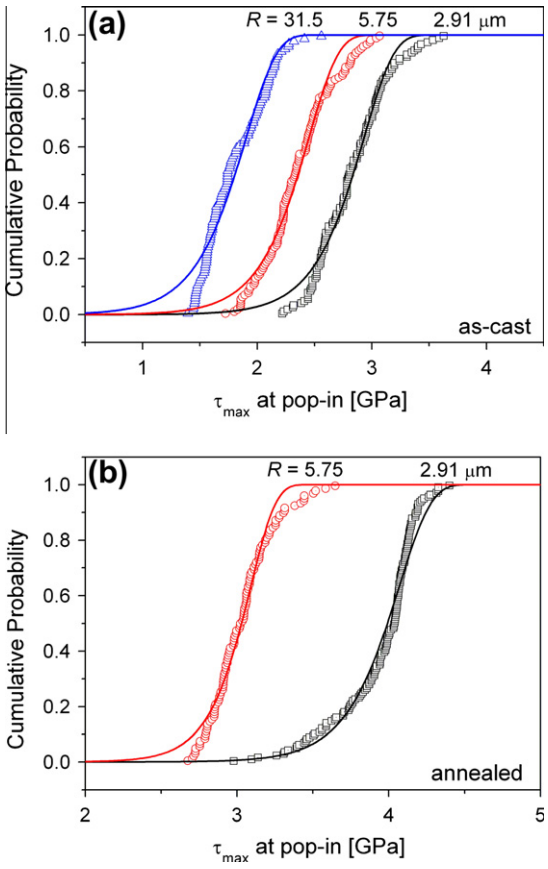

Fig. 6. Cumulative probability distributions of the maximum shear stresses at first pop-in loads for the (a) as-cast and (b) annealed BMG.

where kT is thermal energy (k is the Boltzmann constant, T is the temperature), $\dot{\gamma}_0$ is the attempt frequency (i.e. the frequency of the fundamental mode vibration along the reaction pathway), and ΔF^* and V^* are the Helmholtz activation energy and volume of the event, respectively. Eq. (6) can be rewritten as:

$$\ln[\ln(1-f)^{-1}] = \left\{\frac{\Delta F^*}{kT} + \ln\left[\frac{kT}{V^*(d\tau/dt)}\right]\right\} + \left(\frac{V^*}{kT}\right)\tau. \quad (7)$$

Note that $(d\tau/dt)$ is a constant for nanoindentation tests conducted at a fixed loading rate of dP/dt. Therefore, at $\tau = \tau_{max}$, V^* can be estimated from the slope of $\ln[\ln(1-f)^{-1}]$ vs. τ_{max} plot, as shown in Fig. 7 where the tails of the distribution are excluded (so as to obtain representative values that are not dominated by the tail values). The correlation factor (R^2) for every case of the linear fittings in the Fig. 7 is higher than 0.9.

Values of V^* and Ω obtained from Figs. 6 and 7 are listed in Table 2. By combining these with τ_{CT} and τ_{C0} (determined by Eq. (5)), Ω can be estimated through Eq. (4), which are also listed in Table 2. In turn, the number of atoms in the STZ, N, can be estimated on the basis of dense-packing hard-sphere model of metallic glass with an average atomic radius, $R = (\sum_i^n A_i r_i^3)^{\frac{1}{3}}$. Here, A_i and r_i are the atomic fraction and the atomic radius of each element, respectively [25]. The calculated average atomic radius for the Zr-based BMG used in this study is 0.148 nm.

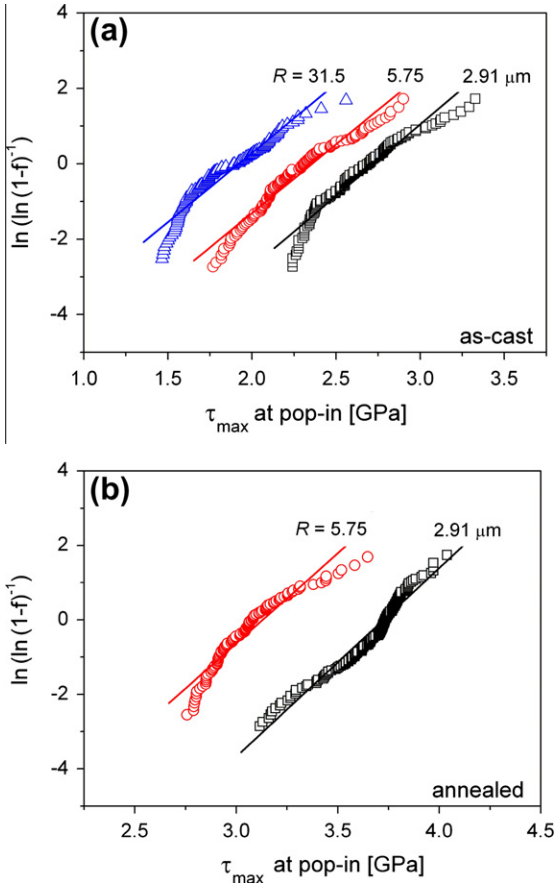

Fig. 7. Linear fits to the $\ln[\ln(1-f)^{-1}]$ vs. τ_{max} data, employed to estimate the STZ size in (a) the as-cast and (b) the annealed BMG.

Table 2
The activation volume and STZ size calculated based on the statistical analysis of the first pop-in data.

Sample	Tip radius, R (μm)	Activation volume, V^* (nm^3)	STZ size	
			STZ volume, Ω (nm^3)	Number of atoms in the STZ, N
As-cast	2.91	0.0156	0.347	26
	5.75	0.0150	0.335	25
	31.5	0.0151	0.337	25
Annealed	2.91	0.0208	0.464	34
	5.75	0.0199	0.443	33

Estimated N values for the BMG in both the structural states examined in this work are listed in Table 2. The fact that the estimated N, which is an intrinsic material parameter, seems independent of the indenter radius, which is an externally imposed experimental variable, supports partly the validity of the above way to estimate the STZ size. The overall range of N (25–34 atoms) is in good agreement with literature data [5–7,26–28]. Computer simulations also reveal local shear events to be of the same size scale [5]. Estimates made by Pan et al. [25] are higher at 200–300 atoms for the STZ in Zr-based BMGs. However, and as discussed below, their analysis was made with rate-dependent hardness data whereas we use the elastic–plastic transition in our analysis.

About 25% increase, from ~25 in the as-cast sample to ~34 in the annealed sample, in the STZ size due to structural relaxation is noted. Intuitively, this appears reasonable; by structural relaxation, free volume decreases and becomes distributed more uniformly, and thus the atoms are somewhat better packed in the annealed sample. Indeed, an increase in mass density (or atomic packing density) of the BMG was observed upon sub-T_g annealing has been reported by Pan et al. [29]. A more uniform structure might be able to engage greater numbers of atoms into collective movement in adjusting to the external stress, the distance to which strains are accommodated (that should be approximately the same as the STZ size) increases.

To the best of our knowledge, only one experimental report is available in the literature on the effect of structural relaxation on STZ size. Pan et al. [29] utilized the strain rate sensitivity, m, of hardness of a Zr–Ni–Cu–Al metallic glass to estimate the STZ size, with a model that is a modified form of CSM. For estimating m, they have utilized the rate-jump nanoindentation tests. Their results show that the STZ size decreases with annealing, which is in contrast to our results. However, it is important to note that their method cannot be adopted for, at least, the BMG examined in this work. Like many other BMGs, at room temperature this BMG (Vit-105) has been reported to be negatively strain rate sensitive ($m < 0$) in compression [30,31] or almost rate insensitive ($m \approx 0$) in spherical indentation [32]. The negative sensitivity is understandable given

the flow localization tendency in them. Additionally, it appears that Pan et al. [29] have not considered the material pile-up in hardness estimation, which is significant in BMG [10] and could have a pronounced effect on the inferred hardness values. This and the fact that $m \leqslant 0$ can make a proper estimation of activation volume from m very difficult. On the contrary, the current work relies on a fairly large amount of robust data and a proven analysis. Thus, an increase in STZ size with structural relaxation appears to be correct and also physically meaningful.

5. Summary and conclusions

The size effect on the yield strength of a Zr-based BMG was investigated by recourse to spherical nanoindentation experiments with different tip radii. Unlike an earlier study, we have conducted a large number of experiments so as to obtain statistically significant data on the load at which the first pop-in occurs. This was then converted into the maximum shear stress underneath the indenter with the help of Hertz's spherical indentation contact mechanics. The experimental results establish an ISE, with the pop-in load increasing with decreasing tip radius, which can be described well by a power law. The size of the STZs in the as-cast and structurally relaxed BMG was estimated through a statistical analysis of the data through a model based on the stress-biased activation fluctuations. The estimated STZ size is about 25 atom clusters and increases to about 34 atoms upon structural relaxation.

Acknowledgements

This research is supported by Basic Science Research Program through the National Research Foundation of Korea (NRF) funded by the Ministry of Education, Science and Technology (No. 2010-0025526). We thank Dr. H. Bei at ORNL for providing the valuable sample.

References

[1] Pharr GM, Herbert EG, Gao Y. Annu Rev Mater Res 2010;40:271.
[2] Nix WD, Gao HJ. Mech Phys Solids 1998;46:411.
[3] Shim S, Bei H, George EP, Pharr GM. Scripta Mater 2008;59:1095.
[4] Morris JR, Bei H, Pharr GM, George EP. Phys Rev Lett 2011;106:165502.
[5] Schuh CA, Hufnagel TC, Ramamurty U. Acta Mater 2007;55:4067.
[6] Argon AS. Acta Metall 1979;27:47.
[7] Argon AS, Shi LT. Acta Metall 1983;31:499.
[8] Jang JI, Yoo BG, Kim YJ, Oh JH, Choi IC, Bei H. Scripta Mater 2011;64:753.
[9] Bei H, Lu ZP, Shim S, Chen G, George EP. Metall Mater Trans A 2010;41:1735.
[10] Yoo BG, Park KW, Lee JC, Ramamurty U, Jang JI. J Mater Res 2009;24:1405.
[11] Lind ML, Duan G, Johnson WL. Phys Rev Lett 2006;97:015501.
[12] Johnson KL. Contact mechanics. Cambridge: Cambridge University Press; 1985.
[13] Oliver WC, Pharr GM. J Mater Res 1992;7:1564.
[14] Liu CT, Heatherly L, Easton DS, Carmichael CA, Schneibel JH, Chen CH, et al. Metall Mater Trans A 1998;29:1811.
[15] Wang L, Bei H, Gao YF, Lu ZP, Nieh TG. Acta Mater 2011;59:7627.
[16] Murali P, Ramamurty U. Acta Mater 2005;53:1467.
[17] Yoo BG, Kim YJ, Oh JH, Ramamurty U, Jang JI. Scripta Mater 2009;61:951.
[18] Wagner H, Bedorf D, Kuchemann S, Schwabe M, Zhang B, Arnold W, et al. Nat Mater 2011;10:439.
[19] Stillinger FH, Weber TA. Science 1995;267:1935.
[20] Harmon JS, Demetriou MD, Johnson WL, Samwer K. Phys Rev Lett 2007;99:135502.
[21] Wang XD, Lou HB, Gong Y, Vainio U, Jiang JZ. J Phys: Condens Matter 2011;23:075402.
[22] Choi IC, Zhao Y, Yoo BG, Kim YJ, Suh JY, Ramamurty U, et al. Scripta Mater 2012;66:923.
[23] Johnson WL, Samwer K. Phys Rev Lett 2005;95:195501.
[24] Schuh CA, Lund AC. J Mater Res 2004;19:2152.
[25] Pan D, Inoue A, Sakurai T, Chen MW. Proc Natl Acad Sci USA 2008;105:14769.
[26] Wang L, Lu ZP, Nieh TG. Scripta Mater 2011;65:759.
[27] Heggen M, Spaepen F, Feuerbacher M. J Appl Phys 2005;97:033506.
[28] Heilmaier M, Eckert J. Adv Eng Mater 2005;7:833.
[29] Pan D, Yokoyama Y, Fujita T, Liu YH, Kohara S, Inoue A, et al. Appl Phys Lett 2009;95:141909.
[30] Dalla Torre FH, Dubach A, Siegrist M, Löffler JF. Appl Phys Lett 2006;89:091918.
[31] Song SX, Bei H, Wadsworth J, Nieh TG. Intermetallics 2008;16:813.
[32] Trichy GR, Scattergood RO, Koch CC, Murty KL. Scripta Mater 2005;53:1461.